Generalized Watershed and PDEs for Geometric-Textural Segmentation

Anastasia Sofou and Petros Maragos

School of Electrical and Computer Engineering, National Technical University of Athens, Greece. Email: `[sofou, maragos]@cs.ntua.gr`

Abstract In this paper we approach the segmentation problem by attempting to incorporate cues such as intensity contrast, region size and texture in the segmentation procedure and derive improved results compared to using individual cues separately. We propose efficient simplification operators and feature extraction schemes, capable of quantifying important characteristics like geometrical complexity, rate of change in local contrast variations and orientation, that eventually favor the final segmentation result. Based on the morphological paradigm of watershed transform we investigate and extend its PDE formulation in order to satisfy various flooding criteria, and couple them with texture information thus making it applicable to a wider range of images.

Keywords: watershed, flooding, multi-cue segmentation, PDEs.

1. Introduction

In this work we treat image segmentation as a set of procedures that need to be followed starting from the initial image and yielding the final partitioning perceived either as a region map or a segmentation boundary. Independently of the method used to achieve the partitioning, this can be divided into the following stages: (i) *image simplification* (ii) *feature extraction* and (iii) *partitioning* into disjoint regions. The simplification stage encompasses tasks such as smoothing, noise reduction, redundant information removal (resulting in an image consisting mostly of flat and large regions), as well as image decomposition into constituent parts. The feature extraction deals with gradient features computation, texture measurements, marker extraction, whereas the final stage of partitioning is the application of the selected segmentation algorithm so as to produce a region map of the image.

Motivated by the efficacy of watershed transform along with latest trends in image segmentation research that encourage combination of different cues [2, 9], we try to incorporate the generalized flooding concept of watershed, thus exploiting intensity contrast and region size criteria [19], with other perceptually meaningful image characteristics such as texture, aiming at improved segmentation results. Additionally, we aim at integrating the aforementioned ideas with Partial Differential Equation (PDE) modeling.

In this paper we propose well-motivated and efficient image simplification and feature extraction techniques as necessary tasks of the presegmentation part. We focus on generalized watershed techniques, investigate their PDE formulation encompassing various flooding criteria, such as region size and volume, and incorporate geometric and textural features in flooding using a leveling-based image decomposition scheme. The resulting segmentation method couples contrast, size and texture information driven by two separate image components: Cartoon U (for contrast information) and Texture component V, resulting from $U + V$ image decomposition model. The modeling is done via PDEs using ideas from curve evolution and level sets, and the implementation is accomplished by adapting specialized level set methodologies, which ensure speed and reduced computational cost. The performance and efficacy of the proposed segmentation scheme is demonstrated through a set of qualitative, quantitative and comparative experimental results.

2. Image Simplification

The simplification stage is concerned with noise and redundant information removal, resulting in an image with smoother structure, but at the same time with key features accurately preserved, easier to handle and more appropriate for further processing such as feature extraction and partitioning. The primary concern here is the selection of the filtering the image has to undergo in order to retain meaningful information but at the same time suppress pointless structures without causing boundary blurring or contour displacement. An efficient family of filters that have the aforementioned properties are the morphological connected operators [11,12,17]. For image simplification we use contrast/area/volume filtering and levelings. Further, generalized openings γ and closings φ are often combined sequentially to produce Alternating Sequential Filters (ASF): $\Psi_{\text{ASF}}(I) = \varphi_n\gamma_n...\varphi_2\gamma_2\varphi_1\gamma_1(I)$, where $i = 1, 2, ...n$ denotes the increasing scale of the filter.

Contrast filtering.The graylevel reconstruction opening ρ^- and closing ρ^+ of an image $I(x, y)$ given a marker signal $M(x, y)$ are:

$$\rho^-(M|I) = \lim_{n\to\infty} F_n,\ F_n = \delta_B(F_{n-1}|I),\ F_0 = M \tag{1}$$

$$\rho^+(M|I) = \lim_{n\to\infty} F_n,\ \ F_n = \varepsilon_B(F_{n-1}|I),\ F_0 = M \tag{2}$$

where $\delta_B(M|I)$ and $\varepsilon_B(M|I)$ denote the conditional dilation and erosion, respectively, of M by a unit disk B constrained by I. To achieve contrast filtering we set the marker $M = I - h$ and $M = I + h$ for reconstruction opening and closing, respectively, with h being a constant that controls the contrast of the bright/dark connected components that will be merged.

Self-Dual filtering. The above operators are either anti-extensive or extensive, simplifying bright or dark image components, respectively. Sym-

metrical simplification of image components requires self-dual filters, such as the **levelings**, which are nonlinear, increasing and idempotent filters that have many interesting scale-space properties [11, 12]. They treat symmetrically the image foreground and background; further, they can be analyzed as composition of reconstruction opening and closing. They operate on a reference image I by locally expanding/shrinking an initial seed image, called the marker M, and globally constraining the marker evolution by the reference image. Specifically, iterations of the image operator $\lambda(F|I) = (\delta(F) \wedge I) \vee \varepsilon(F)$, where $\delta(F)$ (resp. $\varepsilon(F)$) is a dilation (resp. erosion) of F by a small disk, yield in the limit the leveling of I w.r.t. M,

$$\Lambda(M|I) = \lim_{k\to\infty} F_k,\ F_k = \lambda(F_{k-1}|I),\ F_0 = M \tag{3}$$

Levelings preserve the coupling and sense of variation in neighbor image values and do not create any new regional maxima or minima across scales. In practice, they can reconstruct whole image objects with exact preservation of their boundaries and edges. In this reconstruction process they simplify the original image by completely eliminating smaller objects inside which the marker cannot fit.

Area filtering. The need often occurs to filter out small light (respectively dark) particles from graylevel images without damaging the remaining structures. The operator that achieves this kind of filtering is the area opening (closing) of size n that keeps only the light (dark) connected components whose area (number of pixels) is equal or greater than a threshold n. For binary images $X = \bigcup_i X_i$ expressed as disjoint union of connected components X_i, the area opening is $\alpha_n^-(X) = \bigcup\{X_j\ :\ \text{Area}(X_j) \geq n\}$. Dually, the binary area closing is $\alpha_n^+(X) = [\alpha_n^-(X^c)]^c$. The graylevel area opening is defined via threshold superposition:

$$\alpha_n^-(I)(x,y) = \sup\{h\ : (x,y) \in \alpha_n^-(T_h(I))\} \tag{4}$$

where $T_h(I) = \{(x,y) :\ I(x,y) \geq h\}$ are the upper level sets of the image I by thresholding it at level h. Similarly for the graylevel closing.

Volume filtering. A combination of the above contrast and size connected operators yields the volume reconstruction operator. Volume operators remove connected components from the image whose volume is below a certain threshold. They are defined as:

$$\beta_n^-(I)(x,y) = \sup\{h\ : (x,y) \in \beta_n^-(T_h(I))\} \tag{5}$$

$$\beta_n^+(I)(x,y) = \sup\{h\ : (x,y) \in \beta_n^+(T_h(I))\} \tag{6}$$

where in the binary case, if $T_h(I) = X = \bigcup_i X_i$ we define $\beta_n^-(X) = \bigcup\{X_j :$ $\text{Area}(X_j) \cdot h \geq n\}$ with X_j being connected components. Volume operators present the formal properties of openings and closings and can be used as a mean of simplification filtering that balances contrast and size criteria.

3. Feature Extraction

The feature extraction stage deals with the extraction of special image features which facilitate the final segmentation step, and requires a more severe but detailed processing of the image. As *features* we denote regions of interest, gradients, texture measurements, as described below.

Gradient features. High values of the image's gradient are indicative of abrupt intensity changes and specify possible object/region contours. Additionally, the topographic relief, emerging from the gradient magnitude function is used in the flooding process that leads to the final segmentation map. There are many different types of gradients that have been extensively used in the edge detection framework. Among them, we choose the morphological gradient $\mathcal{M}_{\nabla}(I) = [(I \oplus B) - (I \ominus B)]/2$ for its robust behavior low complexity, and better segmentation results compared to other edge strength operators.

Texture features. A way of acquiring texture information from an image I is via a decomposition scheme [13, 21], according to which the image is expressed as $I = U + V$, where U is the "cartoon component" and consists of relatively flat plateaus for the object regions surrounded by abrupt edges, whereas V is the "texture oscillation" and contains texture information plus noise. Simple texture patterns appearing in V component can be modeled as narrowband 2D AM-FM signals [4, 7] of the form $\alpha(x, y)\cos[\phi(x, y)]$, with a spatially varying amplitude $a(x, y)$ and a spatially-varying instantaneous frequency vector $\vec{\omega}(x, y) = \nabla\phi(x, y)$ The amplitude is used to model local image contrast and the frequency vector contains rich information about the locally emergent spatial frequencies. An efficient way to estimate the 2D amplitude and frequency signals is via the 2D Teager energy operator [7] $\Psi(f) \triangleq ||\nabla f||^2 - f\nabla^2 f$. Applying Ψ to the AM-FM signal yields $\Psi[a\cos(\phi)] \approx a^2||\vec{\omega}||^2$, i.e., the product of the instantaneous amplitude and frequency magnitude squared, which may be called the *texture modulation energy*. Complex (wideband) image textures can be modeled as a sum of 2D AM-FM signals; i.e., $f(x, y) = \sum_{k=1} \alpha_k(x, y)\cos[\phi_k(x, y)]$. In our case, Ψ is applied on narrowband versions of the wideband signal V, which are obtained by convolving it with a dense filterbank [4] of 2D Gabor filters h_k. The modulation energies of the filtered texture components are measured via the 2D Energy Operator Ψ, smoothed by a local averaging filter h_a and then are subjected to pixelwise comparisons. This yields the *Maximum Average Teager Energy* $\Psi_{\text{mat}}[f(x, y)] = \max_k h_a * \Psi[f * h_k](x, y)$. It is a slowly-varying indication of texture modulation energy, which can classify among different energy levels. It provides both local and global texture information and tracks the most dominant texture components along multiple modulation bands [5]. The derived image texture feature is capable of quantifying important characteristics like geometrical complexity, rate of change in local contrast variations and texture scale.

Markers. Markers are predefined image locations that serve as start-

ing points of the region-growing procedure. These seed points grow in time according to a set of specified criteria until the image plane is totally covered by them. It is common practice that markers are chosen as regions where some homogeneity criterion is constant or a key characteristic is of certain strength. In our research work we emphasize on contrast, volume and texture-based markers, i.e., image areas where the homogeneity criterion is contrast, volume (area and contrast) and texture, respectively. In all three cases we extract markers via a reconstruction procedure as valleys or peaks of an image transform that resembles one of the aforementioned characteristics. In all cases, the scale is incorporated in the structuring element or reconstruction controlling parameter. Specifically, we distinguish the following cases:

Contrast , Area or Volume - based markers. Markers are estimated as valleys (or peaks) of certain strength of a generalized Bottom (Top) Hat Transform. The Bottom Hat Transform is defined as: $H_B(I) = \varphi(I) - I$, where $\varphi(I)$ is a generalized closing and I is an intensity image (initial or simplified). Similarly, Top Hat Transform is defined as: $H_T(I) = I - \gamma(I)$, where $\gamma(f)$ is a generalized opening. Depending on what kind of closing /opening transform we choose, we obtain: (a) *contrast* markers if the generalized closing is based on reconstruction, i.e $\varphi(I) = \rho^+(I + h|I)$ that is where the parameter h controls the contrast (valley depth), (b) *area* markers if $\varphi(I)$ is area closing, (c) *volume* markers if $\varphi(I)$ is volume closing, in which case contrast and area criteria are exploited.

Texture - based markers. Again markers are estimated as peaks of an image transform that relies on texture characteristics. Therefore, peaks (valleys) either of the texture component V or its dominant modulation energy are extracted as highly (poorly) textured regions. The peak (valley) extraction is based on a reconstruction procedure as discussed earlier.

4. Generalized Watershed and PDEs

Apart from the standard morphological flooding approach implemented either via immersion simulations [22] or hierarchical queues [1], the watershed transform has also been modeled in a continuous way via the eikonal PDE [14] and implemented in [8] using curve evolution and level sets. Further, generalized floodings and corresponding watersheds have been investigated in [10]. Using a PDE-based modeling in the flooding process of watershed transform, each emanating wave's boundary is viewed as a curve, which evolves with predefined speed. In the case of uniform height watershed flooding, let us consider a moving smooth closed curve, which is the boundary of the marker region, $\vec{C}(p,t)$ where $p \in [0,1]$ parameterizes the curve and t is an artificial marching parameter. The PDE that implements the generalized watershed flooding is:

$$\frac{\partial \vec{C}}{\partial t} = \frac{c}{\text{Area}(t)\|\nabla I\|} \cdot \vec{N} \tag{7}$$

where c is a constant, $\|\nabla I\|$ is the gradient magnitude of the image function I, $\vec{N}$ is the unit outward vector normal to the curve, and Area(t) is either 1 if we perform only contrast-based segmentation (height flooding) or Area(t) = Area$(\vec{C})$, that is Area(t) is equal to to area enclosed by the propagating curve at the specific time t in case of contrast and size segmentation (volume flooding) [19]. The above propagation PDE implies that the evolution speed is inversely proportional to the intensity (volume) variation at each image point, in the direction of the outward normal vector. For implementation we use the level set approach [15] where at each time the evolving curve is embedded as the zero level set $\Gamma(t) = \{(x, y) : \Phi(x, y, t) = 0\}$ of a higher dimension space-time function $\Phi(x, y, t)$. Then this embedding function Φ evolves in space-time according to the following PDE:

$$\frac{\partial \Phi}{\partial t} = \frac{c}{\text{Area}(t)\|\nabla I(x, y)\|}\|\nabla \Phi\| \tag{8}$$

Modeling generalized watersheds via the eikonal has the advantage of a more isotropic flooding but it also introduces some challenges in the implementation. Efficient algorithms [18] to solve time-dependent eikonal PDEs are the narrow-band level sets methods, and more specifically, the fast marching method, an algorithm for stationary formulations of eikonal PDEs.

Experimental results using height and volume flooding segmentation of Eq.(7) are illustrated in Fig. 1, exploiting the basic property of volume flooding, i.e., retaining the balance between area and contrast. The image shown left in Fig. 1 is synthetically produced by taking the distance transform of the corresponding binary image and adding an arbitrary constant to each of their connected components. For illustration purposes, a flooding source has been superimposed for each object. Bright objects appear with higher altitude compared to darker objects. Next in Fig. 1 we illustrate the contour lines of each object, with blue color corresponding to lower altitude and red corresponding to higher altitude. The cases of uniform height and volume flooding are examined and presented in third and fourth column of Fig. 1, respectively. In the case of height flooding the object of lowest contrast is totally lost, whereas in the case of volume flooding the undetected object is the one of lowest volume (area and contrast).

5. Coupled Contrast - Texture Segmentation

The aforementioned generalized watershed segmentation schemes use as prominent characteristic the image intensity viewed either as seeds' contrast, size or volume. Any textural information present in the image is incorporated in intensity. Based on evidence from psychophysics according to which humans combine multiple cues in order to detect boundaries from images [16], we try to exploit contrast and texture as two separate information sources so as to improve and balance the segmentation results and eliminate false boundaries introduced by intensity variations in amplitude and phase,

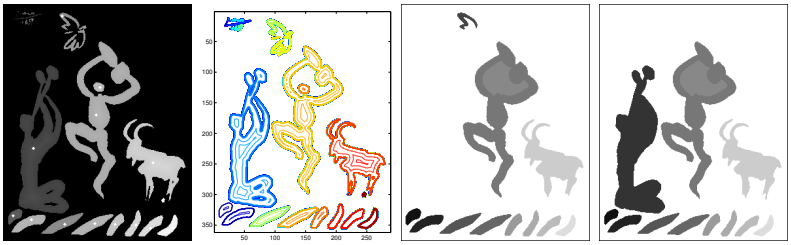

Figure 1. **Height and Volume Flooding Segmentation Results**: (from left to right) synthetic image, contours corresponding to different altitudes (gray values), (height flooding segmentation regions, volume flooding segmentation regions.

owing to textured parts. Ideally we want to add a texture-controlled term to the height/flooding PDE (7) that will be able to quantify properly the available image texture information by enabling the growing seeds surpass false edges introduced by texture structures in the image, thus speeding up the evolution at such places. This can be achieved by the Ψ_{mat} operator, which provides both local and global texture information, tracks the most dominant texture components along multiple modulation bands and is capable of quantifying important characteristics like geometrical complexity, rate of change in local contrast variations and texture scale. We thus conclude to the following PDE:

$$\frac{\partial \vec{C}}{\partial t} = \left(\frac{\lambda_1}{\max(\epsilon, \text{Area}(t)||\nabla I||)} + \lambda_2 \Psi_{\text{mat}}(I) \right) \vec{N} \tag{9}$$

λ_1 and λ_1 are parameters that control the contribution of each cue and $0 \leq \epsilon \leq 1$ is used to handle instabilities caused by gradient's zero values. The seeds' evolution speed depends on two eikonal terms, linked with some optimality criterion. The first term drives the curve (seed's boundary) with speed that maximizes the *flooding* of the image toward its watershed. The second term can be shown to correspond to a flow that maximizes the average texture energy: $\max \iint_{R(C)} \Psi(I) \Longrightarrow \partial \vec{C}/\partial t = \Psi(I)\vec{N}$. This term pushes the curve toward regions with large average texture energy.

The PDE (9) consists of two terms: the gradient magnitude operator quantifying intensity changes and the energy modulation operator quantifying AM-FM variations corresponding to texture. Our next concern is to apply these two different operators of separate image transformations emphasizing on different type of information. We take advantage of the recently proposed image decomposition model [13, 21], which provides an effective way of linearly distinguishing contrast and texture from a single image, in the form $I = U + V$. Specifically, the U component, known as *cartoon*, serves very well as a contrast descriptor since it consists of relatively flat plateaus that correspond to object regions, surrounded by abrupt edges that correspond to object boundaries. The V component, which is in fact

the *texture oscillation* contains texture oscillations plus noise information and serves as texture descriptor. Combining the $U+V$ image decomposition philosophy with the PDE (9) and level set formulation [15] we derive the following coupled segmentation PDEs:

$$\frac{\partial \vec{C}}{\partial t} = \left(\frac{\lambda_1}{\text{Area}(t)||\nabla U||} + \lambda_2 \Psi_{\text{mat}}(V) \right) \vec{N} \tag{10}$$

$$\frac{\partial \Phi}{\partial t} = \left(\frac{\lambda_1}{\text{Area}(t)||\nabla U||} + \lambda_2 \Psi_{\text{mat}}(V) \right) \ ||\nabla \Phi|| \tag{11}$$

Contrast variations are taken into account from the U part, which is obtained by applying the leveling operator on the initial image and texture oscillations are approached through the residual $V = I - U$. The elimination of division-by-zero scenario as introduced in Eq.(9) can be as well applied in Eq.(11) and Eq.(11) in order to handle instabilities.

In the PDE derived above each cue's contribution is controlled by a coefficient, namely λ_1 geometric evolution controlling parameter and λ_2 texture evolution controlling parameter. We set these λ parameters to be spatially adaptable, taking advantage of the fact that the $U + V$ image decomposition model gives evidence about the existence of each component (geometry and texture) at every image location. All the needed information about contrast at each image pixel is encapsulated by $1/|\nabla U|$ component and texture contribution is captured by $\Psi_{\text{mat}}(V)$. Hence, we estimate λ_1 (geometric coefficient) and λ_2 (textural coefficient) as the mean square error between the observed image I and the texture V or contrast U component, respectively. These mean square errors are weighted locally by a small Gaussian window $G_\sigma(x, y)$ of scale σ, i.e., $\lambda_1(x, y) = [G_\sigma * (I - V)^2](x, y)$ and $\lambda_2(x, y) = [G_\sigma * (I - U)^2](x, y)$. We can either use this estimated λ-space functions directly or normalize their sum to 1. Alternatively, the coefficients can be estimated as: $\lambda_1(x, y) = \exp(-[G_\sigma * (I - U)^2](x, y))$ and $\lambda_2(x, y) = \exp(-[G_\sigma * (I - V)^2](x, y))$. The former selection of λ parameters has experimentally been found to yield slightly better results.

The curves that propagate according to the aforementioned evolution scheme are multiple, initialized as the contours of a set of markers, thus indicating significant image regions. The marker extraction is done according to the methodologies described in 3. Specifically, depending on the type of image to be segmented we choose our markers to be contrast-oriented, texture-oriented, a combination of the above or manually placed at areas of interest. The PDE (11) is of pure eikonal-type and its implementation is based on established techniques from level sets methods, specifically the fast marching methodology (FMM) [18],[20] that ensures computational speed.

6. Experiments, Comparisons, and Conclusions

In Fig. 2 we demonstrate a set of the extracted features and segmentation results on a biomedical image from prostate tissue used for gleason scale measurement. The reference image is shown left on top row of Fig. 2. In same row we illustrate the automatically extracted marker set, U and V image components obtained after image decomposition. In the second row we illustrate the texture modulation energies $\Psi_{\text{mat}}(I)$, and $\Psi_{\text{mat}}(V)$, as well as the corresponding segmentation results using PDEs (9) and (11).

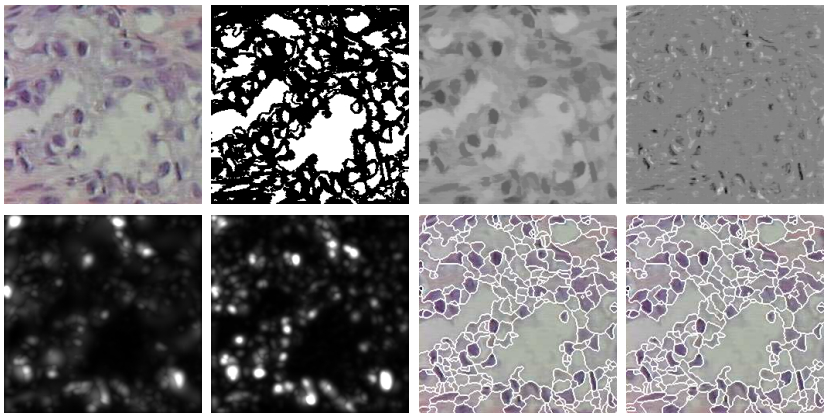

Figure 2. **Image Features and Segmentation Results**:(from left to right) Original image, Markers, Cartoon U, Texture V, Texture modulation energy $\Psi_{\text{mat}}(I)$, Texture modulation energy $\Psi_{\text{mat}}(V)$, Coupled segmentation on I, Coupled segmentation on $U+V$.

In order to judge the quality of the obtained segmented images, we have used some quality measures in order to quantify the results and test them against other segmentation methodologies. Although there is a variety of goodness criteria for the evaluation of segmentation methodologies, and each criterion can be used in different segmentation scenarios, there is no global measure that can be applied in every case. Among the goodness measures [23] established according to human perception and intuition, we eventually concluded to measure each region intensity variance using a cartoon version of the image, as well as each region's modulation energy variance, thus incorporating both contrast and texture information. The lower those variance values, the better are the segmentation results.

The proposed method was tested against height and volume flooding watershed segmentation, as well as the multicue scheme without image decomposition of Eq.(9), since these methods produce similar segmentation results in terms of closed boundaries and disjoint, plane-filling regions.

In Fig. 3, we provide a set of different segmentation results obtained by applying the aforementioned methods on four different reference images:

1) a soilsection image consisting of highly contrasted and textured areas, 2) an aerial photo 3) a biomedical image of prostate tissue and 4) an animal image of differently textured areas. The different segmentation methodologies are tested using the same set of automatically extracted markers via contrast or volume criteria for each image (in the case of the animal image markers are placed manually). Marker sets' illustration is omitted due to lack of space. Apart from visual comparisons, we provide Table 1, where the aforementioned goodness measures are computed for each case. As it can be observed, the proposed scheme incorporating image decomposition outperforms the other segmentation methodologies. It provides better results, in the sense that the resulting partitioning map consists of more uniform regions (low cartoon variance values) with smoother texture (low modulation energy variance), compared to the other methodologies.

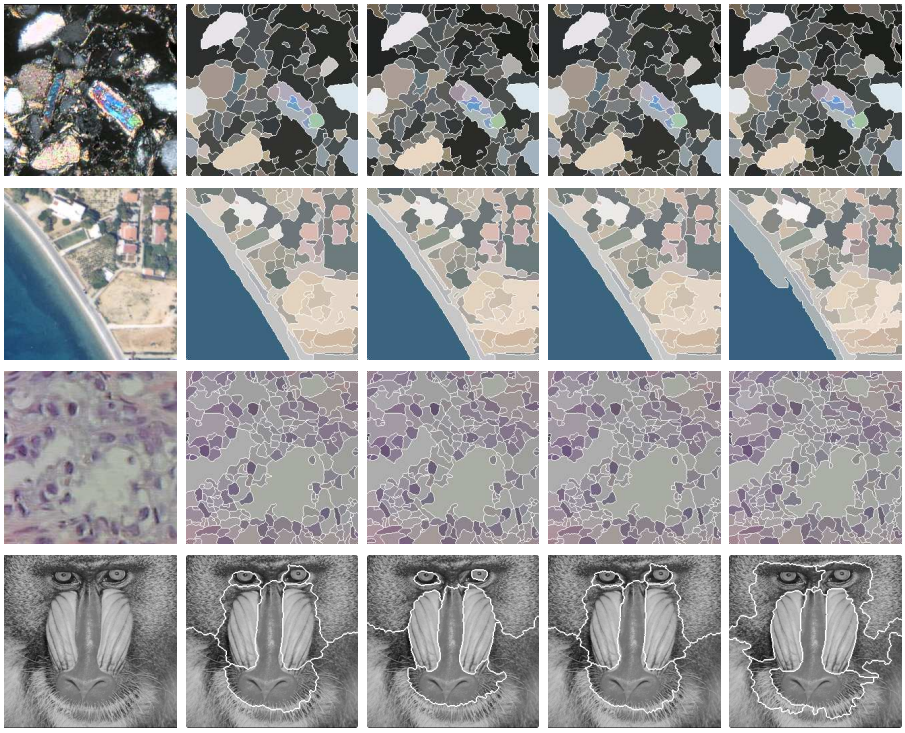

Figure 3. **Comparisons of different types of watershed-like segmentation results**: (Columns from left to right) Reference images, Multicue segmentation results without decomposition, Multicue segmentation results with decomposition, Height watershed flooding segmentation results, Volume watershed flooding segmentation results.

Concluding Remarks: The presented research work addressed the

Table 1. Segmentation Comparisons

	Quality Measures	Segmentation Method			
		Coupled Type		Watershed Flooding	
		I	U+ V	Height	Volume
soil	var(U)	0.921	0.823	0.893	1.108
	var(Ψ_{mat}(V))	0.280	0.259	0.281	0.254
	length(Γ)	4855	4987	4982	5742
aerial	var(U)	0.335	0.281	0.337	0.383
	var(Ψ_{mat}(V))	0.473	0.468	0.479	0.555
	length(Γ)	3934	4206	4054	4442
biomed	var(U)	0.327	0.294	0.314	0.365
	var(Ψ_{mat}(V))	0.138	0.135	0.140	0.139
	length(Γ)	6529	6630	6728	7593
madrill	var(U)	0.046	0.024	0.046	0.034
	var(Ψ_{mat}(V))	0.272	0.232	0.271	0.285
	length(Γ)	1167	1210	1201	1960

problem of image segmentation in terms of simplification, feature extraction and image partitioning with focus on a generalized flooding procedure using geometric and textural information. Generalized watershed transform was modeled via PDEs and extended to incorporate geometric and textural information using ideas such as $U+V$ image decomposition and texture AM-FM modeling. The quality of segmentation results was illustrated through qualitative, quantitative and comparative results.

It should be noted that geometric curve evolution of the form $\partial\vec{C}/\partial t = g(c - \mu\kappa)\vec{N}$ has been proposed by Caselles et al [3] and Malladi et al [6]. However, our proposed scheme has three differences compared to the aforementioned evolution: i) it has a term that achieves watershed type flooding ii) it has a second term that is a new contribution and acts on the texture component of the image that, to our best knowledge, has never been used before in segmentation schemes, and iii) the curvature component κ is not present in our scheme since it was experimentally determined that it does not provide any significant improvement to the overall segmentation.

Acknowledgments: This research work was supported by the project PYTHAGORAS (of EPEAEK II) which is co-funded by the European Social Fund (75%) and the Greek National Resources (25%). The authors also wish to thank G. Evangelopoulos for his valuable help in the texture analysis part and G. Papandreou and S. Lefkimmiatis for help with pdfLaTeX.

References

[1] S. Beucher and F. Meyer, *The Morphological Approach to Segmentation: The Watershed Transformation*, Mathematical morphology in image processing, 1993.

[2] T. Brox, M. Rousson, R. Deriche, and J. Weickert, *Unsupervised Segmentation Incorporating Colour, Texture, and Motion*, Computer Analysis of Images and Patterns, 2003, pp. 353–360.

[3] V. Caselles, R. Kimmel, and G.Sapiro, *Geodesic Active Contours*, Int'l J. Comp. Vision **22** (1997), no. 1, 61–79.

[4] J. P. Havlicek, D. S. Harding, and A. C. Bovik, *The Multi-component AM-FM Image Representation*, IEEE Trans. Image Processing **5** (1996), no. 6, 1094–1100.

[5] I. Kokkinos, G. Evangelopoulos, and P. Maragos, *Advances in Texture Analysis: Energy Dominant Components and Multiple Hypothesis Testing*, Proc. ICIP, 2004.

[6] R. Malladi, J. A. Sethian, and B. C. Vemuri, *Shape modeling with front propagation: A level set approach*, IEEE Tr. Pattern Anal. Mach. Intel. **17** (1995), no. 2, 158–175.

[7] P. Maragos and A. C. Bovik, *Image Demodulation Using Multidimensional Energy Separation*, J. Opt. Soc. Amer. A **12** (1995), no. 9, 1867–1876.

[8] P. Maragos and M. A. Butt, *Curve evolution, differential morphology, and distance transforms applied to multiscale and eikonal problems*, Fundamenta Informaticae **41** (2000), 91 –129.

[9] D. Martin, C. Fowlkes, and J. Malik, *Learning to Detect Natural Image Boundaries Using Local Brightness, Color, and Texture Cues*, IEEE Tr. Pattern Anal. Mach. Intel. **26** (2004), no. 5, 530 –549.

[10] F. Meyer and P. Maragos, *Multiscale morphological segmentations based on watershed, flooding, and eikonal pde*, Proceedings of scale-space, 1999, pp. 351–362.

[11] ———, *Nonlinear scale-space representation with morphological levelings*, J. Visual Communications. & Image Representation **11** (2000), 245–265.

[12] F. Meyer, *The Levelings*, Proc. fourth international symposium on mathematical morphology and its applications to image processing, 1998June, pp. 199 –206.

[13] Y. Meyer, *Oscillating Patterns in Image Processing and Nonlinear Evolution Equations*, University Lecture Series, vol. 22, AMS, 2002.

[14] L. Najman and M. Schmitt, *Watershed of a continuous function*, Signal Processing **38** (1994), no. 7, 99–112.

[15] S. Osher and J. Sethian, *Fronts propagating with curvature-dependent speed: Algorithms based on hamilton-jacobi formulations*, J. Comp. Phys. **79** (1988), 12–49.

[16] J. Rivest and P. Cavanagh, *Localizing contours defined by more than one attribute*, Vision Research **36** (1996), no. 1, 53 –66.

[17] P. Salembier and J. Serra, *Flat zones filtering, connected operators, and filters by reconstruction*, IEEE Trans. Image Processing **4** (1995), no. 8, 153–1160.

[18] J. A. Sethian, *Level set methods and fast marching methods*, Cambridge University Press, 1999.

[19] A. Sofou and P. Maragos, *PDE-based Modeling of Image Segmentation using Volumic Flooding*, Proc. Int'l Conf. Image Processing, 2003.

[20] J. N. Tsitsiklis, *Efficient algorithms for globally optimized trajectories*, IEEE Trans. Automat. Contr. **40** (1995), no. 9, 1528–1538.

[21] L. A. Vese and S. J. Osher, *Modeling textures with total variation minimization and oscillating patterns in image processing*, J. Sci. Comp. **19** (2003), no. 1-3, 553–572.

[22] L. Vincent and P. Soille, *Watershed in digital spaces: An efficient algorithm based on immersion simulations*, IEEE Tr. Pat. Anal. Mach. Intel. **13** (1991June), 583–598.

[23] Y. J. Zhang, *A survey on evaluation methods for image segmentation*, Pattern Recognition **29** (1996), no. 8, 1335–1346.